The supra-long Scots pine tree-ring record for Finnish Lapland: Part 2, interannual to centennial variability in summer temperatures for 7500 years

Samuli Helama, Markus Lindholm, Mauri Timonen, Jouko Meriläinen and Matti Eronen

The Holocene 2002; 12; 681
DOI: 10.1191/0959683602hl581rp

The Holocene 12,6 (2002) pp. 681–687

The supra-long Scots pine tree-ring record for Finnish Lapland: Part 2, interannual to centennial variability in summer temperatures for 7500 years

Samuli Helama,[1]* Markus Lindholm,[1] Mauri Timonen,[2] Jouko Meriläinen[3] and Matti Eronen[1]

([1]Department of Geology, PO Box 64, FIN-00014 University of Helsinki, Finland; [2]Finnish Forest Research Institute, PO Box 16, FIN-96301 Rovaniemi, Finland; [3]Saima Centre for Environmental Sciences, University of Joensuu, Linnankatu 11, FIN-57130 Savonlinna, Finland)

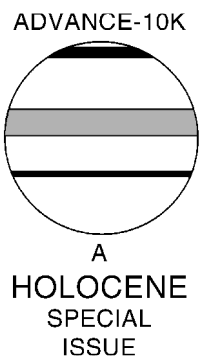

Abstract: Midsummer (July) temperatures are reconstructed for the last 7500 years using the long ring-width chronology of Scots pine (*Pinus sylvestris* L.) from northern Finland. The chronology was built using regional curve standardization (RCS), which allows for long-term (low-frequency) variability to be extracted from this annually resolved record of 1087 samples from living trees and subfossil timber. Short- and long-term changes in reconstructed July temperatures are presented. The regression model accounts for 37% of the dependent instrumental temperature variance between AD 1879 and 1992. The warmest 30-year periods were AD 560–531, AD 560–531, 1190–1161 BC and AD 1541–1570, and the coldest 5240–5211, 5150–5121 and 3710–3681 BC. The warmest 100-year periods were AD 1501–1600, 600–501 BC and 300–201 BC, and the coldest 5200–5101, 2500–2401 and 1500–1401 BC. Broad comparisons are made with dendrochronological, lacustrine and glacial proxy evidence.

Key words: Dendroclimatology, tree rings, summer temperature, *Pinus sylvestris*, Finnish Lapland, Holocene.

Introduction

In this work, northern Finnish Lapland midsummer (July) temperatures are reconstructed for the last seven and a half millennia using the many absolutely dated tree-ring-width series of Scots pine (*Pinus sylvestris* L.) described by Eronen *et al.* (this issue).

A climatic reconstruction based on a single chronology is spatially more restricted in its regional representation than a series of separate local reconstructions that might be produced using networks of ring-width and density chronologies, perhaps comprised of various tree species (e.g., Fritts, 1976). However, by combining the regional information within a single series we are able to produce an extended series, and we give special attention here to the extraction of the lowest possible frequencies of variability contained in the multitude of individual tree records in an attempt to represent timescales of summer-temperature variability ranging from one to several hundred years. This information is especially valuable during recent millennia as a regional context within which to analyse the variability that has been observed during the most recent century.

*Author for correspondence (e-mail: samuli.helama@helsinki.fi)

Material and methods

Tree-ring and climate data

A decade of sampling, data preparation, measurement and cross-dating activities that make up the recent history of dendrochronological activities in Finnish Lapland is described by Eronen *et al.* (this issue). The number of living trees used here to construct the 'modern' section of the chronology was limited to 50, in order that the recent era should not be over-sampled. Beside these 50 living trees (Lindholm, 1996; Lindholm *et al.*, 1996) the chronology contains data from a further 1041 samples from dead standing logs and subfossil wood recovered from small lakes (Eronen *et al.*, this issue), 1081 tree-ring series in all. Samples from living trees from three distinct areas were selected, based on geographical distribution and the variety of tree ages.

The climate data were taken from two meteorological stations: Karasjok in Norway and Karesuando in Sweden. The arithmetic mean of these stations was used, starting from the year of 1879, which is the earliest available year of instrumental temperature measurements from both of the stations.

10.1191/0959683602hl581rp

Chronology construction and reliability

In order to remove the innate bias in the measured tree-ring records, attributable to growth trend through the life of the tree, and to preserve as much low-frequency variation in the chronology as possible, we have applied the regional chronology standardization (RCS) method of detrending the initial tree-ring records prior to their incorporation within the composite mean chronology. Standardization is the process of transforming measured ring-width series into series of indices, i.e., deviations from the underlying growth/age model (Fritts, 1976). This RCS is based on the idea that trees growing within a relatively geographical and ecological homogeneous region, and of the same species, share a single idealized model of ring growth as a function of tree age. This function can be accurately calculated if a sufficient number of trees are used and individual variations suppressed by the law of averages (Huntington, 1914). This concept was applied to standardize tree-ring time series in Swedish Lapland as early as in the 1930s by Erlandsson (1936), and was later discussed by Fritts (1976). The technique was re-adopted by Briffa *et al.* (1992; 1996) where it was termed the RCS-standardization technique, and described in the specific context of capturing tree-growth changes on long timescales, i.e., low-frequency variation.

Applying the time-invariant RCS growth model (defined using data from a long period of time) as the expectation of ring width at any particular tree age allows the overall level of tree growth at any particular time to systematically over- or underestimate the curve when external growth influences, such as a shift in climate, cause the rate of tree growth to exceed or underestimate the 'expected rate' on the tree growth anomaly. This deviation will be preserved in the indexed series, potentially overcoming the 'segment length curse' described by Cook *et al.* (1995), where evidence of such changes are not distinguishable from internal tree-growth effects and are effectively removed, the more so when the external changes occur over periods that exceed the length of the tree-ring records. Briffa *et al.* (1992) noted that there may be several sources of potential error in the application of the RCS procedure. For example, when deriving the empirical evidence of the age/growth function, it is sometimes difficult to assign the exact biological age to each ring since the individual series only seldom begin at the pith (Norton and Ogden, 1990). This can be especially problematic for subfossil logs, which are not often preserved intact in the lake sediment. In such a case, it is quite impossible to sample at the usual breast height, as is done in the case of living trees. Here we are forced to follow Briffa *et al.* (1992) in assuming that the first measured ring of each series corresponds to the theoretical first year of tree growth.

As a measure of the strength of the common growth 'signal' within the chronology and to estimate chronology reliability, we have calculated the mean interseries correlation (RBar) and the expressed population signal (EPS), that quantifies the similarity between the averaged chronology (the mean of a finite number of sample indices) and the theoretical 'infinitely replicated' chronology (i.e., an EPS of 1.0) for the appropriate Rbar (Wigley *et al.*, 1984). RBar was calculated over a moving 30-year window using the mean tree-series available within the window. RBar values run from 5511 BC, when this replication was a minimum of four series.

Climatic calibration and verification

The relationship between climate and the radial growth of Scots pine in this region has been explored previously, and repeatedly the average temperature of concurrent July has been found to be the strongest determining or growth-limiting factor, when only ring width is considered (e.g. Erlandsson, 1936; Hustich, 1948; Briffa *et al.*, 1988, 1990; Lindholm, 1996; Lindholm *et al.*, 1996; Lindholm and Eronen, 2000; Gervais and MacDonald, 2000). As pines in the region show relatively high autocorrelation (Table 1), the growth in year t depends on the climate also in previous years t–n. This effect can be exploited by considering the climate in year t to be a function of tree growth in years concurrent with growth but also potentially up to (n) years preceding and (n) years following ring formation (Fritts, 1962; Fritts *et al.*, 1971; Briffa *et al.*, 1988; Lindholm and Eronen, 2000). Linear multiple regression (Fritts, 1976) is used to estimate this relationship. Here, July regional temperature was modelled using linear multiple regression with the chronology values for year t and those for up to three previous and three following years offered as potential predictors, the final model being chosen using a stepwise selection procedure with entry and removal criteria for retention of predictors set at an F probability of less than 0.05 and 0.10 respectively.

A cross-calibration/verification procedure, similar to that used by Briffa *et al.* (1988; 1990), was adopted. The full overlap time period of tree-ring and climate data was divided into two 57-year periods, 1879–1935 and 1936–92, and each used to fit and then verify the calibrated equation: early calibrated/late verified and late calibrated/early verified, respectively.

Age-dependent growth functions

Two separate age/growth (RCS) functions were empirically derived, one based on 'modern' and one on subfossil pines. Both are well modelled as negative exponential curves, though with different curvature. The formulae for the curves are presented in a form following Fritts *et al.* (1969) as:

$$\text{Modern } (RCS_{ra}) = 0.9405e^{-0.0062t} + 0.2014 \quad (1)$$

$$\text{Subfossil } (RCS_{re}) = 0.9137e^{-0.1252t} + 0.2559 \quad (2)$$

where t is the cambial age. The very first years of the modern and subfossil time series show rather similar values of growth (in millimetres). However, after ages of about 10 years, the ring widths of modern series appear to decline more slowly until the cambial age reaches proximally 400 years, after which the declining trends are virtually parallel, with expected growth equal in old age. The similarity of growth in the early years can be interpreted as indicative of accurate sampling and preparation of the material used. However, the slower decline in ring width with age seen in the more modern time series might reflect reduced environmental stress on dry land compared to near-shore habitat, or somewhat less severe growing conditions over the shorter period in which the modern trees grew, compared to those that prevailed over the longer timespan represented by the subfossil data.

If the former supposition is true, the use of separate RCS curves to detrend the measured data will remove a potential bias in the modern part of the chronology. If the latter supposition is true, the use of the later RCS curve will potentially remove evidence of a modern climate shift.

Results

Tree-growth responses to climatic factors

When the RCS chronology is correlated against individual mean monthly temperatures (during 1879–1992) and monthly precipitation totals (1901–90), July mean temperature displays the highest ($p<0.01$) association in both subperiods (Table 1). This result is in agreement with the previous studies of the same species in this region cited earlier. The RCS chronology also displays significant ($p<0.01$) first-order autocorrelation, and to a lesser extent ($p<0.05$) second-order autocorrelation, again shown consistently in both subperiods.

The instrumental July temperature record contains no significant autocorrelation. The highest and lowest recorded values are 17.7°C and 8.5°C respectively. The greatest first-difference values

Table 1 Correlations between the pine ring-width chronology and July mean temperature (Karesuando and Karasjok) over the calibration period. The calibration period is divided into two subperiods. Significant correlations at the 0.05 level (*) and at the 0.01 level (**) are shown. A1 and A2 denote autocorrelations of order one and two in the chronology

a) temperature	previous year						concurrent year								A1	A2
	J	A	S	O	N	D	J	F	M	A	M	J	J	A		
1879–1935	0.29*	0.09	0.09	0.08	0.29*	0.28*	0.26	0.05	0.01	0.07	0.26	0.13	0.55**	0.17	0.84**	0.71**
1936-1992	−0.14	0.01	−0.03	−0.07	0.11	0.23	0.22	−0.09	0.19	0.06	0.09	0.17	0.43**	0.30*	0.51**	0.33*

b) precipitation	previous year						concurrent year							
	J	A	S	O	N	D	J	F	M	A	M	J	J	A
1901–1945	0.00	0.14	0.11	0.22	−0.01	0.30*	0.04	0.15	0.30*	0.2	0.31*	0.09	−0.19	−0.04
1946-1990	−0.17	−0.02	0.16	−0.15	−0.14	0.21	0.21	−0.08	−0.18	−0.04	0.27	−0.07	−0.26	0.06

Table 2 Calibration and verification statistics for the reconstruction. The calibration period (1879–1992) is divided into two subperiods for cross-validation. Significance at p<0.01 level is denoted by two asterisks (**)

Calibration period	1879–1935	1936–1992	1879–1992
Verification period	1936–1992	1879–1935	
Calibration			
Variance explained	0.410	0.347	0.373
Verification			
Variance explained	0.341	0.387	
Reduction of error	0.323	0.381	
Coefficient of error	0.310	0.368	
Sign test			
Correct	38**	39**	
Incorrect	18	17	
Regression weights			
TRW_t	1.068	0.646	0.976
TRW_{t+1}	−0.614	−0.459	−0.620

(i.e., those between any consecutive pair) occurred between 1900 and 1901 when the mean July temperature fell by 7.1°C.

The statistics summarizing the calibration and verification of the July temperature prediction equation are summarized in Table 2. The results of the independent verification comparison of actual against estimated temperatures show that 34 and 39% of the dependent (predictand) temperature variance was explained over the separate verification periods. Reduction of error (RE) and coefficient of efficiency (CE) statistics are positive for both subperiods indicating real skill in the reconstruction (Fritts *et al.*, 1990; Briffa *et al.*, 1988). The First Difference Sign Test results (Fritts, 1976) are also significant at p=0.01 level for both verification subperiods. The magnitude of the coefficients in the separate regression equations do vary slightly but the final form of the equation is the same with predictors for only growth year *t* and *t*+1 retained. They are large and positive on the current year *t*, and negative and smaller for the subsequent growth year (*t*+1). The alternate calibration-period reconstructions have more than 97.5% variance in common over the period of available instrumental data.

A final reconstruction equation was recalibrated, using the entire period of overlapping instrumental and tree-ring data. This resulted in a transfer function of the following form:

$$\text{July } T_t = 0.976 * RCS_t - 0.620 * RCS_{t+1} \quad (3)$$

where T_t is the mean July temperature in year *t*, and RCS_t and RCS_{t+1} are the ring-width indices for the years *t* and *t*+1, respectively.

Table 3 The largest abrupt changes in summer temperatures in northern Finnish Lapland. The first differences between consecutive years in the record were arranged in descending order. DIFF refers to this difference in degrees Celsius

Years	DIFF
BC 1585–1584	9.02
AD 535–536	7.95
AD 1600–1601	7.32
BC 331–330	7.17
BC 1583–1584	7.17
AD 535–534	7.00
BC 2565–1564	6.78
AD 39–40	6.58
BC 535–534	6.52
BC 533–534	6.51

Short- and long-term temperature changes

Reconstructed average July temperatures are presented in Figure 1: short-timescale variations in the uppermost plot; decadal to centennial variations in the middle plot; and non-overlapping century-length means in the lower histogram. The upper plot effectively represents Fritts (1976). The lower-frequency variation is expressed using a 100-year smoothing spline (Cook and Peters, 1981). The average reconstructed mean July temperature over the full calibration period is 13.15°C (SD=2.98°C) and the mean of the entire reconstruction period 12.68°C (SD=1.08°C). The observed mean July temperature is twice that for the April-through-August mean. This can be used as a guideline for comparing these results with reconstructions of the longer season.

Table 3 shows the largest abrupt shifts between adjacent years in reconstructed July temperatures and the top part of Table 4 lists the coldest and warmest individual summers. The warmest midsummer was experienced in AD 535 and the coldest in 1584 BC. These represent the largest and fifth largest high-frequency shifts in the entire record. The latter year appears also in the list (Table 3) of the most prominent shifts, bracketed by the second and sixth greatest shifts.

Other extreme periods of various lengths are listed in Tables 4 and 5. Table 5 shows the most extreme intervals of 1000 years. The warmest and coldest 10-year, non-overlapping periods occurred in 530–521 BC and 2030–2021 BC, respectively. Three

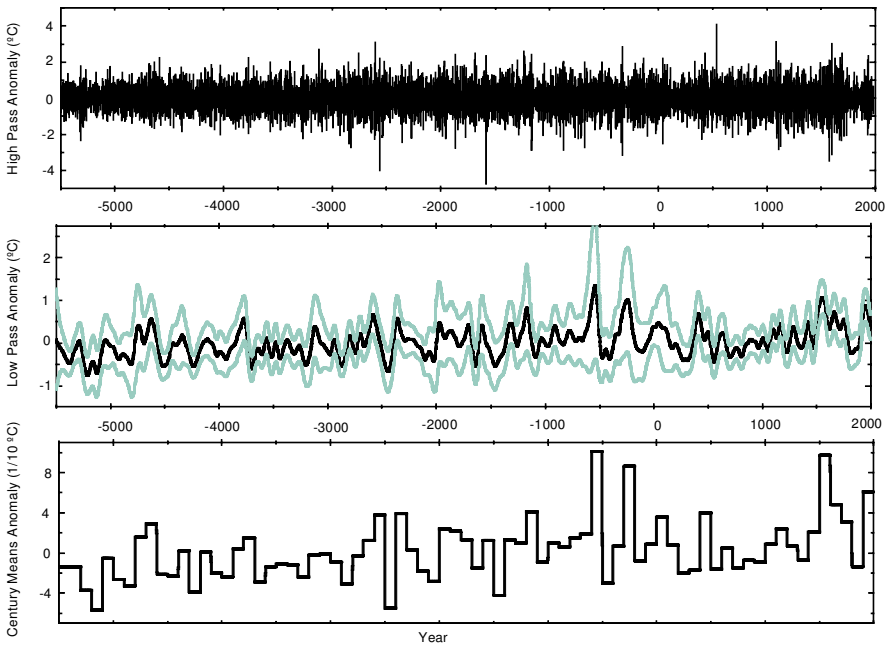

Figure 1 Reconstructed July mean temperature anomalies (°C) presented as high (< 8 years, upper plot) and low-frequency (>8 years, middle plot) with corresponding 95% confidence limits (middle plot). Non-overlapping 100-year means of century-wise midsummer temperatures are shown at the bottom.

of the eight warmest 10-year periods occurred during the sixth century BC. A list of non-overlapping 30-year intervals is shown in Table 4, where two periods from this century appear. The warmth of the sixth century BC is also emphasized in Table 5, where the warmest of all (overlapping) 30-year periods occurred during 533–524 BC. In addition, the warmth of the sixteenth century AD is clearly evident and the twentieth century AD is represented by the 30-year period starting in 1930 (Table 4); this is also the warmest of the overlapping periods shown in Table 5. It is notable that all the most severe non-overlapping 30-year periods shown in Table 4 occurred in the years before Christ.

The warmest and coldest non-overlapping 100-year periods are reconstructed here as AD 1501–1600 and 5200–5101 BC, respectively. The sixteenth century AD is also followed by a warm seventeenth century, the fourth warmest in Table 4. Between these, in terms of rank, are also the warm sixth and third centuries BC, with the severe cold period, 484–385 BC seen between them in Table 5. Again, all the centennial non-overlapping coolest periods fall within the years BC. The coldest period after Christ falls in the third century, though it is only the 17th coldest of the whole record.

Discussion

Comparisons with other tree-ring reconstructions

Briffa *et al.* (1990; 1992) produced tree-ring-based reconstructions of summer-temperature changes in northern Sweden, and Briffa *et al.* (1995) presented a reconstruction for northern Siberia, on the eastern side of the Urals. These reconstructions are only between one and two thousand years long and the comparison here must be restricted to common time periods. However, similar features in these reconstructions are observed regardless of partly different standardization methods, geographical distance, and difference in the precise reconstructed season.

The correlation between the present chronology and that of Briffa *et al.* (1992), for AD 601–1980, is 0.19. Centuries of the most significant ($p<0.001$) correlation are the fifteenth, seventeenth, nineteenth and twentieth AD. The centuries with the poorest correlation are the seventh and sixteenth centuries AD, both of them having correlations of only 0.05.

The severity of the cool year AD 1601 (Tables 4 and 5) was also noted by Briffa *et al.* (1992; 1995) and linked to the eruption of the Huaynaputina volcano in Peru. Other evidence of this cold from a wide network of tree-ring-density chronologies in North America and Europe is also found in Jones *et al.* (1995) and Briffa *et al.* (1998).

The warmth reconstructed here for AD 1561–1570 overlaps with the warm 20-year period previously reported in northern Sweden (Briffa *et al.*, 1995). Coinciding with reported warmth in northwest Siberia (Briffa *et al.*, 1995) are our warm periods in AD 1541–1570 and 1931–1960. The former interval also overlaps with the period recorded by Briffa *et al.* (1990; 1995), and is generally found as the last warm decade of the overall warm sixteenth century AD in north European tree-ring chronologies (Briffa *et al.*, 1999).

The warmth of the seventeenth century AD reconstructed here is not, however, seen in previous reconstructions based on Swedish or Russian tree-ring data (e.g., Briffa *et al.*, 1992; 1995; 1999; 2001). Instead, they describe a lowering of summer temperatures in these regions, and averaged over the Northern Hemisphere as a whole.

Comparison with other proxy records

Korhola *et al.* (2000) have produced a reconstruction of July temperature change based on the statistical calibration of diatom data, partly in the same region as this study. The timespan of their reconstruction was the same as that here, but it should be noted that their lake sediments do not provide the same degree of high-resolution definition as is provided by tree-ring data. The comparisons between their reconstructions and those presented here are limited to a potential range of timescales between several decades and multiple centuries. According to their study, a major cold episode occurred over a period of several hundred years, centred at around 7200 cal. yr BP. Though our reconstruction does not indicate a consistent cool excursion of this duration, this span of time is still prominent in Tables 4 and 5, the coolest centennial period of all being reconstructed here at 5208–5109 BC (Table 5). In the diatom-based reconstruction, the warmest conditions influencing this region during the Holocene are evident between 7000 and 5000 cal. yr BP. The RCS-based tree-ring reconstruction indicates century-long warmth between 3841 and 3742 BC (Table 5).

Table 4 Extreme midsummer (July) temperatures in northern Finnish Lapland based on temperature reconstruction. Individual years as well as various periods are presented. DEP refers to temperature departure from the long-term reconstruction mean

Warmest years	DEP	Coldest years	DEP
The most anomalous individual years			
AD 535	6.17	BC 1584	–5.00
BC 547	5.60	BC 2564	–4.28
AD 1089	4.92	BC 330	–3.78
BC 1165	4.67	BC 2850	–3.58
BC 3123	4.60	BC 874	–3.33
BC 560	4.53	AD 1601	–3.27
AD 1694	4.48	BC 738	–3.25
BC 2604	4.44	AD 1574	–3.21

Warm periods	DEP	Cold periods	DEP
10-year non-overlapping intervals			
BC 530–521	2.33	BC 2030–2021	–1.27
BC 1170–1161	2.02	BC 5140–5131	–1.22
AD 401–410	1.72	BC 420–411	–1.17
BC 550–541	1.65	AD 541–550	–1.17
BC 240–231	1.58	BC 4480–4471	–1.06
AD 1651–1660	1.49	BC 330–321	–1.05
BC 590-581	1.43	BC 5130–5121	–1.04
AD 1561–1570	1.36	BC 2120–2111	–1.03
30-year non-overlapping intervals			
BC 560–531	1.42	BC 5240–5211	–0.85
BC 1190–1161	1.33	BC 5150–5121	–0.83
AD 1541–1570	1.11	BC 3710–3681	-0.79
BC 260–231	1.04	BC 5210–5181	–0.71
AD 1931–1960	1.02	BC 1670–1641	–0.69
AD 1571–1600	1.00	BC 2990–2961	–0.67
BC 530–501	0.94	BC 3950–3921	–0.66
AD 1511–1540	0.90	BC 2450–2421	–0.65
100-year non-overlapping intervals			
AD 1501–1600	0.99	BC 5200–5101	–0.60
BC 600–501	0.97	BC 2500–2401	–0.59
BC 300–201	0.83	BC 1500–1401	–0.45
AD 1901–1992	0.61	BC 4300–4201	–0.42
AD 1601–1700	0.41	BC 5300–5201	–0.40
BC 1200–1101	0.38	BC 4900–4801	–0.37
BC 2400–2301	0.36	BC 2900–2801	–0.34
AD 401–500	0.36	BC 5400–5301	–0.33

However, this period does not show such clearly discernible additional warmth in the perspective of the entire reconstruction. The fall and the minima of temperatures approximately between 4500 and 2800 cal. yr BP (Korhola *et al.*, 2000) is marked particularly in the twenty-fifth and fifteenth centuries BC. The minimum phase of midsummer temperature they reconstruct is coincident with the cold phase reconstructed here in 2500–2401 BC (Tables 4 and 5), the second harshest century in our reconstruction. This also corresponds to the date of an ice-rafting episode documented from North Atlantic deep sea cores by Bond *et al.* (1997).

Karlén (1988; 1991) has compiled evidence of glacier-size variations in northern Sweden over the last nine millennia, drawn from historical records, radiocarbon dating of wood, lichenometric dates on moraines, and changes in the composition of sediments in proglacial lakes. Karlén (1991) also made a comparison of his glacier record with local tree-ring evidence over the last 15 centuries. Five of the eight coldest tree-ring-derived centuries, the fifty-second, twenty-fifth, forty-third, fifty-third and fifty-fourth centuries BC, overlap with periods of glacial advance in Karlén's (1988) curve. There are even clearer parallels with the centennial cool periods in Table 5. The most notable simultaneous cold intervals apparent in both records occurred in 5208–5109 BC, 2500–2401 BC, 484–385 BC and AD 1812–1911. All other centennial intervals recorded in Table 5 overlap at least partly with glacial advances.

Conclusions

There has been an emphasis in this work on expressing longer timescales of temperature variability than have been shown in previous work based on the northern Finnish subfossil tree-ring data. A basic assumption of the RCS method used here to achieve this is that of homogeneity within the sample data, in terms of ecological source region and with respect to maintaining sufficient samples through time (Briffa *et al.*, 1992; 1996). The present data do not entirely meet these requirements, but it is hoped that future sampling will boost the sample replication to provide a major improvement in the robustness of the chronology trends.

Table 5 Midsummer (July) temperature extremes: for individual years and periods of various length, in consecutive millennia during the reconstructed period. DEP refers to temperature departure from long-term reconstruction mean

Warmest intervals	**BC 5520–4001**	**BC 4000–3001**	**BC 3000–2001**	**BC 2000–1001**	**BC 1000–1**	**AD 1–1000**	**AD 1001–1992**
Individual year	BC 4590	BC 3123	BC 2604	BC 1165	BC 547	AD 535	AD 1089
DEP	3.48	4.60	4.44	4.67	5.60	6.17	4.92
10-year period	BC 4720–4711	BC 3132–3123	BC 2366–2357	BC 1171–1162	BC 533–524	AD 403–412	AD 1930–1939
DEP	1.25	1.43	1.24	2.18	2.71	1.75	1.70
30-year period	BC 4653–4624	BC 3771–3742	BC 2611–2582	BC 1190–1161	BC 551–522	AD 406–435	AD 1558–1587
DEP	0.72	0.84	0.91	1.33	1.83	0.89	1.19
100-year period	BC 4688-4589	BC 3841–3742	BC 2622–2523	BC 1238–1139	BC 604–505	AD 28–127	AD 1501–1600
DEP	0.41	0.46	0.47	0.54	1.04	0.46	0.99
Coldest intervals	**BC 5520–4001**	**BC 4000–3001**	**BC 3000–2001**	**BC 2000–1001**	**BC 1000–1**	**AD 1–1000**	**AD 1001–1992**
Individual year	BC 5321	BC 3053	BC 2564	BC 1584	BC 330	AD 824	AD 1601
DEP	–2.98	–3.16	–4.28	–5.00	–3.78	–2.92	–3.27
10-year period	BC 5138–5129	BC 3453	BC 2024–2015	BC 1649–1640	BC 420–411	AD 542–551	AD 1813–1822
DEP	–1.55	–1.05	–1.53	–1.07	–1.17	–1.33	–0.90
30-year period	BC 5138–5109	BC 3712–3683	BC 2459–2430	BC 1648–1619	BC 422–393	AD 542–571	AD 1459–1488
DEP	–-1.08	–0.81	–0.86	–0.77	–0.68	–0.78	–0.56
100-year period	BC 5208–5109	BC 3250–3151	BC 2500–2401	BC 1506–1407	BC 484–385	AD 221–320	AD 1812–1911
DEP	–0.67	–0.44	–0.59	–0.47	–0.35	–0.42	–0.22

Our measurement series are drawn from the forest limit region so the growth of the trees is largely unaffected by stand competition and disturbances, due to the relatively wide spacing between trees. This increases the likely reliability of our empirically defined age/growth function that is used as the basis for removing age-related trends in the measurement data. As Fritts (1976) pointed out, the use of a single growth curve in this way in only valid for studies at somewhat unusual environments, e.g., at the tree-line or polar limit.

However, we found a slight difference between the growth curves of modern and subfossil data, and thus separate curves were used for these particular sets of series in standardization. In the original sample data base, the number of modern trees is far greater than the number generally available for earlier periods of time. The number of living trees was reduced to 50, constituting three individual site chronologies (Lindholm, 1996). The sites represent the eastern, western and northern parts of the overall region of subfossil material collection. However, the chronology sample replication over the entire length of the record requires further enhancement as it is clearly far from optimal. The number of constituent series is inadequate for making definite conclusions about longer-term (>century) trends in growth variability in the entire region of northern Fennoscandia. Sample depth remains consistently above 25 only for the last 14 centuries. Despite the use of the RCS approach, the reconstruction presented here does not indicate significant temperature trends on millennium timescales. The improved reconstructions of interannual to centennial scales of variance may still need to be combined with evidence on longer timescales derived from other temperature proxies to provide a more complete spectrum of temperature variations in this and other regions during the Holocene.

Acknowledgements

Besides the early support of ADVANCE-10K (under grant ENV4-CT95-0127) this work was funded by the Academy of Finland (grant 40962 to Matti Eronen) and another EC research project, EXTRATERRESTRIAL (ERBIC15CT980123). We acknowledge the careful measurement of ring widths by several assistants in various laboratories.

References

Bond, G., Showers, W., Cheseby, M., Lotti, R., Almasi, P., deMenocal, P., Priore, P., Cullen, H., Hajdas, I. and **Bonani, G.** 1997: A pervasive millennial-scale cycle in North Atlantic Holocene and glacial climates. *Science* 278, 1257–66.

Briffa, K.R., Bartholin, T.S., Eckstein, D., Jones, P.D., Karlén, W., Schweingruber, F.H. and **Zetterberg, P.** 1990: A 1,400-year tree-ring record of summer temperatures in Fennoscandia. *Nature* 346, 434–39.

Briffa, K.R., Jones, P.D., Bartholin, T.S., Eckstein, D., Schweingruber, H.F., Karlén, W., Zetterberg, P, and **Eronen, M.** 1992: Fennoscandian summers from AD 500: temperature changes on short and long timescales. *Climate Dynamics* 7, 111–19.

Briffa, K.R., Jones, P.D., Pilcher, J.R. and **Hughes, M.K.** 1988: Reconstructing summer temperatures in northern Fennoscandia back to AD 1700 using tree-ring data from Scots pine. *Arctic and Alpine Research* 20, 385–94.

Briffa, K.R., Jones, P.D., Schweingruber, F.H., Karlén, W. and **Shiyatov, S.G.** 1996: Tree-ring variables as proxy-climate indicators: problems with low-frequency signals. In Jones, P.D., Bradley, R.S. and Jouzel, J., editors, *Climatic variations and forcing mechanisms of the last 2000 years*, NATO ASI Series, vol. I 41, Berlin: Springer-Verlag, 9–41.

Briffa, K.R., Jones, P.D., Schweingruber, F.H. and **Osborn, T.J.** 1998: Influence of volcanic eruptions on Northern Hemisphere over the past 600 years. *Nature* 393, 450–55.

Briffa, K.R., Jones, P.D., Schweingruber, F.H., Shiyatov, S.G. and **Cook, E.R.** 1995: Unusual twentieth-century summer warmth in a 1,000-year temperature record from Siberia. *Nature* 376, 156–59.

Briffa, K.R., Jones, P.D., Vogel, R.B., Schweingruber, F.H., Baillie, M.G.L., Shiyatov, S.G. and **Vaganov, E.** A. 1999: European tree-rings and climate in the 16th century. *Climatic Change* 43, 151–68.

Briffa., K.R., Osborn, T.J., Schweingruber, F.H., Harris, I.C., Jones, P.D., Shiyatov, S.G. and **Vaganov, E.** 2001: Low-frequency temperature variations from a northern tree ring density network. *Journal of Geophysical Research* 106(D3), 2929–41.

Cook, E.R. and **Peters, K.** 1981: The smoothing spline: a new approach to standardizing forest interior tree-ring series for dendroclimatic studies. *Tree-Ring Bulletin* 41, 45–53.

Cook, E.R., Briffa, K.R., Meko, D.M., Graybill, D.A. and **Funkhouser, G.** 1995: The 'segment length curse' in long tree-ring chronology development for palaeoclimatic studies. *The Holocene* 5, 229–37.

Cook, E.R., Briffa, K.R., Shiyatov, S.G. and **Mazepa, V.** 1990: Tree-ring standardization and growth-trend estimation. In Cook, E.R. and Kairiukstis, L.A., editors, *Methods of dendrochronology: applications in the environmental sciences,* Dordrecht: Kluwer Academic Publishers, 104–23.

Erlandsson, S. 1936: *Dendrochronological studies*. Report 23. Uppsala, Sweden: Stockholms Högskolas Geokronological Institute.

Fritts, H.C. 1962: An approach to dendroclimatology: screening by means of multiple regression techniques. *Journal of Geophysical Research* 67, 1413–20.

—— 1976: *Tree rings and climate*. London: Academic Press, 567 pp.

Fritts, H.C., Blasing, T.J., Hayden, B.P. and **Kutzbach, J.E.** 1971: Multivariate techniques for specifying tree-growth and climate relationships and for reconstructing anomalies in paleoclimate. *Journal of Applied Meteorology* 10, 845–64.

Fritts, H.C., Guiot, J. and **Gordon, G.A.** 1990: Verification. In Cook, E.R. and Kairiukstis, L., editors, Methods of dendrochronology: applications in the environmental science, Dordrecht: Kluwer Academic Publishers, 178–85.

Fritts, H.C., Mosimann, J.E. and **Bottorff.** 1969: A revised computer program for standardizing tree-ring series. *Tree-Ring Bulletin* 29, 15–20.

Gervais, B.R. and **MacDonald, G.M.** 2000: A 403-year record of July temperatures and treeline dynamics of *Pinus sylvestris* from Kola Peninsula, Northwest Russia. *Arctic, Antarctic, and Alpine Research* 32, 295–302.

Huntington, E. 1914: The climatic factor as illustrated in arid America. Carnegie Institution Publication 192, Washington.

Hustich, I. 1948: The Scotch pine in northernmost Finland and its dependence on the climate in the last decades. *Acta Botanica Fennica* 42, 1–75.

Jones, P.D., Briffa, K.R. and **Schweingruber, F.H.** 1995: Tree-ring evidence of the widespread effects of explosive volcanic eruptions. *Geophysical Research Letters* 22, 1333–36.

Karlén, W. 1988: Scandinavian glacial and climatic fluctuations during the Holocene. *Quaternary Science Reviews* 7, 199–209.

—— 1991: Glacier fluctuations in Scandinavia during the last 9000 years. In Starkel, L., Gregory, K.J. and Thornes, J.B., editors, *Temperate paleohydrology*, New York: John Wiley, 395–412.

Korhola, A., Weckström, J., Holmström., L. and **Erästö, P.** 2000: A Quantitative Holocene climatic record from diatoms in Northern Fennoscandia. *Quaternary Research* 54, 284–94.

Lindholm, M. 1996: Reconstruction of the past climate from ring-width chronologies of Scots pine (*Pinus sylvestris* L.) at the northern forest limit in Fennoscandia. Publications in Sciences 40. PhD thesis, University of Joensuu.

Lindholm, M. and **Eronen, M.** 2000: A reconstruction of mid-summer temperatures from ring-widths of Scots pine since AD 50 in northern Fennoscandia. *Geografiska Annaler* 82A, 527–35.

Lindholm, M., Timonen, M. and **Meriläinen, J.** 1996: Extracting mid-summer temperatures from ring-width chronologies of living pines at the northern forest limit in Fennoscandia. *Dendrochronologia* 14, 99–113.

Norton, D.A. and **Ogden, J.** 1990: Problems with the use of tree rings in the study of forest population dynamics. In Cook, E.R. and Kairiukstis, L.A., editors, Methods of dendrochronology: applications in the environmental sciences, Dordrecht: Kluwer Academic Publishers, 284–88.

Wigley, T.M.L., Briffa, K.R. and **Jones, P.D.** 1984: On the average value of correlated time series, with applications in dendroclimatology and hydrometeorology. *Journal of Climate and Applied Meteorology* 23, 201–13.